Waste Management 184 (2024) 82–91

Contents lists available at ScienceDirect

Waste Management

journal homepage: www.elsevier.com/locate/wasman

Research Paper

The enrichment and transformation mechanism of Pb and Cu in suspension magnetization roasting and magnetic separation from iron tailings

Guoqiang Qiu, Xunan Ning *, Dingyuan Zhang, Jinhuan Deng, Yi Wang

Guangdong Key Laboratory of Environmental Catalysis and Health Risk Control, School of Environmental Science and Engineering, Guangdong University of Technology, Guangzhou 510006, PR China

ARTICLE INFO

Keywords:
Copper
Lead
Metal enrichment
Phase transformation

ABSTRACT

Magnetic iron concentrate (MIC) and nonmagnetic tailings (NT) are obtained from magnetization roasting of iron tailings (IT). MIC containing Pb adversely affects blast furnace ironmaking, while Cu in NT poses leaching risks. This study utilizes fast pyrolysis-suspension magnetization roasting to recover iron from IT. The enrichment of Pb, Cu, and the phase transformation mechanism of Cu in the process of suspension magnetization roasting and magnetic separation were clarified. Results show 96.13 % of Cu in IT is in limonite and 47.23 % of Pb is associated with iron. At 750 °C, with 10 % dosage of biomass pyrolysis and 10 min roasting, Pb, Cu and Fe contents in MIC are 0.96, 2.14 and 3.17 times that of NT. Increasing roasting temperature enhances Cu associated with iron enrichment into the MIC, while oxidation of free copper oxide associated with iron forms magnetic copper ferrite. Increased pyrolyzed biomass leads to over-reduction of magnetite associated with Cu to FeO associated with Cu, promoting magnetic copper ferrite decomposition into FeO and free copper oxide. This research holds significant importance in controlling the quality of MIC and the storage risk of IT, and provides theoretical guidance for the regulation and recovery of valuable metals in subsequent processes.

1. Introduction

World resources are estimated to be greater than 800 billion tons of crude ore containing more than 230 billion tons of iron (U.S.G.S, 2023). The tailings are the byproducts of ore beneficiation and serve as a primary constituent of industrial solid waste (Bing et al., 2018; Roy et al., 2020). As of 2018, China's iron tailings (IT) production exceeded 10 billion tons, with a comprehensive utilization rate of only about 27.69 % (Zhang, N. et al., 2021). In 2019, the average iron grade of Chinese iron ore decreased by nearly 4 percentage points to 26.62 % compared with 2011 (Yuan et al., 2022). IT are often stored for a long time, occupying vast land resources and leading to acidic mine drainage containing high levels of heavy metals, causing pollution to nearby soils and groundwater (Li et al., 2018; Lyu et al., 2019; Vasile et al., 2021).

Magnetization roasting and direct reduction have emerged as effective methods for iron recovery from IT in recent years, producing high-value iron products (Cheng et al., 2023; Zhang et al., 2022). Compared to direct reduction, magnetization roasting requires lower temperatures and shorter processing times, making it a cost-effective option for the recovery of iron from refractory iron ores (Li et al., 2010; Wu et al., 2018). By providing appropriate temperature and reduction conditions, magnetization roasting can transform weakly magnetic minerals into strongly magnetic ones, realizing efficient magnetic separation from other substances (Deng et al., 2022; Zhu et al., 2020). Sun et al. (2019) used siderite as a reducing agent, siderite can produce CO during decomposition, and iron recovery was achieved through magnetization roasting at a temperature of 700 °C. Deng et al. (2022) used sawdust as a reducing agent and conducted magnetization roasting of IT at 650 °C, obtaining an magnetic iron concentrate (MIC) with a grade of 62.04 % and a recovery rate of 95.29 %. The magnetization roasting technologies typically involve vertical furnaces, rotary kilns, and fluidized bed roasting. Suspension magnetization roasting, as a fluidized bed roasting technique, allows small-sized tailings particles to efficiently undergo phase transformation in a dispersed state, resulting in superior product quality in a shorter time (Cheng et al., 2023; Yu et al., 2019). Cao et al. (2021) utilized straw as the reducing agent in suspension magnetization roasting, obtaining an MIC with a grade of 71.07 % and a recovery rate of 94.17 % at 800 °C. Liu et al. (2022) and Yuan et al. (2020) applied reducing gas and suspension magnetization roasting to obtain a MIC and manganese concentrate. The choice of reducing agents in magnetization

* Corresponding author.
E-mail address: Ningxunan666@gdut.edu.cn (X. Ning).

https://doi.org/10.1016/j.wasman.2024.05.034
Received 22 December 2023; Received in revised form 18 May 2024; Accepted 22 May 2024
Available online 25 May 2024

roasting studies is diverse, with all selections grounded in the magnetization reaction of reducing gases generated by these reducing agents under pyrolysis conditions. These reducing agents encompass reducing gases, biomass, coal, and other ores capable of generating reducing gases (Bagatini et al., 2021; Chen et al., 2022; Nunna et al., 2020; Zhao and Wei, 2020). The details concerning reducing agents, roasting conditions, iron grade, and iron recovery rate utilized in studies related to magnetization roasting for iron recovery are presented in Table S1. Biomass, being a natural carbon source, effectively reduces carbon emissions, promoting green and sustainable development (Nwachukwu et al., 2021; Zhang et al., 2020).

In our previous work, we successfully recovered iron efficiently from IT through fast pyrolysis-suspension magnetization roasting, obtaining MIC with a grade exceeding 60 % (Qiu et al., 2023). MIC serves as one of the raw materials for blast furnace ironmaking, containing certain amounts of valuable metals, which can impact the furnace during the smelting process (Mustafa et al., 2023). Pb poses a risk to the blast furnace as liquid lead permeates the furnace body, causing oxidation expansion and detrimental effects (Jiao et al., 2016; Trinkel et al., 2017). Meanwhile, as one of the valuable metals with minor impact on blast furnace ironmaking, magnetization roasting may affect the phase composition of Cu, thereby influencing the leaching risk of Cu. Studies have shown that copper oxide is more readily leached by acid compared to copper sulfide (Cao et al., 2009). In comparison to CuO, $CuFe_2O_4$ and combined copper oxide exhibit a higher resistance to acid corrosion (Li et al., 2011; Wang et al., 2019). Therefore, understanding the phase transformation mechanism of Cu after magnetization roasting and the mechanism of phase enrichment of Cu in MIC and nonmagnetic tailings (NT) after magnetic separation will contribute to the subsequent exploration of the leaching risk of Cu in MIC and NT. Beauchemin et al. (2020) found the potential sequestration of the main transition metal contaminants −Cu and Ni- into the magnetic phases. Cu in MIC can be transferred to steel by blast furnace smelting, and the corrosion resistance of steel can be significantly improved with a Cu content of less than 0.5 % (Dengler et al., 2000; Hong et al., 2012). At present, the research focus of magnetization roasting is mainly on the transformation and recovery of iron, with MIC as the main research object. There is a lack of comprehensive analysis regarding the reduction characteristics, causation, enrichment patterns and phase transitions of other valuable metals present in IT, magnetized product (MP), MIC and NT. Various valuable metals exist in different mineral occurrence forms in IT, and their corresponding calcination and reduction properties differ significantly. Under conditions of high temperature, not only iron but also other valuable metals undergo corresponding transformations in their chemical forms and enrichment trends.

This study is based on fast pyrolysis-suspension magnetization roasting. The distribution of Fe, Al, Si, Pb, and Cu in IT at different particle sizes, the liberations of limonite and hematite in IT, and the mineral occurrence forms of Pb and Cu in IT were studied. The enrichment ratios of Pb, Cu, and Fe during the suspension magnetization roasting under various temperatures and dosages of biomass pyrolysis were investigated. The phase transformation mechanism of Cu after suspension magnetization roasting and the phase enrichment mechanism of Cu in MIC and NT after magnetic separation were studied. The distribution of Pb in MIC and NT after magnetic separation was described through the mineral occurrence forms of Pb in IT and the mineral association of Pb and Fe in IT. The quality of MIC and the industrial application of fast pyrolysis-suspension magnetization roasting are evaluated. The results of this research hold significant importance in controlling the quality of MIC and the storage risk of NT, and are expected to provide theoretical guidance for the regulation and recovery of valuable metals in subsequent processes.

2. Materials and methods

2.1. Materials

In this study, the IT employed for suspension magnetization roasting was obtained from the storage area of tailings at Dabaoshan in Guangdong. The total Fe (TFe) content of IT was determined to be 43.38 %, and the composition of iron phases is presented in Table. S2. The fast pyrolysis gas was obtained from sawdust of Chinese fir. The chemical composition of the sawdust was determined in our previous studies (Qiu et al., 2023). The contents of total S, Pb and Cu in the IT are 1.07 %, 0.15 % and 0.19 %. The content of total S in the Chinese fir is 0.03 %.

2.2. Methods

2.2.1. Experimental apparatus and procedure

15 g of uniformly mixed IT with a particle size of −10 mesh was loaded into a small vertical suspension furnace, which was then connected to a high-temperature tube furnace. Both furnaces were raised to the required temperature. The mass of biomass was determined as a percentage of the mass of the IT. The reaction system was purged with N_2, and then the biomass was pyrolyzed in the high-temperature tube furnace. During the pyrolysis process, the N_2 flow rate was maintained at 200 mL/min, and the reducing gas produced during pyrolysis followed the N_2 into the small vertical suspension furnace for magnetic roasting reactions. After a reaction time of 10 min, the MP was cooled to room temperature in flowing N_2, and then ground until 100 % could pass through a 200-mesh sieve. Subsequently, continuous wet magnetic separation with a magnetic separation intensity of 120–80-60 mT was used to separate the MIC and NT from the MP

To determine the enrichment effect of valuable metals after magnetic separation, the enrichment ratio, which is the ratio of the metal content in the MIC to the metal content in the NT was used. The enrichment ratio was calculated as follows in Equation (1):

$$E = \frac{c_{MIC}}{c_{NT}} \quad (1)$$

where E is the enrichment ratio of the valuable metal, c_{MIC} is the metal content in the MIC, and c_{NT} is the metal content in the NT.

2.2.2. Analytical tests

Titanium (III) chloride reduction potassium dichromate titration methods (routine methods) were used to measure the TFe content of the MIC and NT. The samples were digested using a microwave digestion system (Coolpex; Preekem, China) according to Method 3052 (EPA, 1996). The content of valuable metals in the digested solutions was measured using an atomic absorption spectrophotometer (TAS-990F; Persee, China). The samples were fixed in the mixed glue of epoxy resin and triethanolamine, polished with a metallographic sample polishing machine (MoPao3s; Veiyee, China). The microstructure of the samples was observed using a scanning electron microscope (SEM, FEI-Tecnai G2, USA). The mineral composition in the IT was determined from the analysis of 152 g of IT using an automated mineral liberation analyzer (MLA), the MLA analysis system is MLA-250, consisting of a scanning electron microscope (SEM, FEI Quanta 650, USA) and an energy dispersive X-ray spectrometer (EDX, Bruker xFlash 5010, Germany), which can provide the boundary of the mineral in the backscattered electron (BSE) mode. X-ray diffraction (XRD, Bruker D8 Advance, Germany) was performed using a Japanese Rigaku SmartLab 9 kW, with the diffraction angle range (2θ) of 10° to 70°, and the scanning rate was kept at 10°/min. HSC Chemistry 5.0 software (HSC, Outokumpu Research Oy, Finland) was employed to carry out conventional thermodynamic calculations based on the minimization of the Gibbs free energy. These calculations were used to evaluate the possible effects of dosage of biomass pyrolysis and temperature on the conversion of valuable metals

during the magnetization roasting.

0.5 g of the sample was weighed and the phase of Cu in IT, MP, MIC and NT was determined using chemical phase analysis. Corresponding extractants (NH_4HF_2, Na_2SO_3, HCl, HNO_3, H_2SO_4, thiourea) were employed for the extraction and determination of a series of Cu mineral phases (free copper oxide, secondary copper sulfide, iron-manganese combined copper oxide, other combined copper oxide, and primary copper sulfide) (Xiao-Feng et al., 2016; Zhang, H. et al., 2021). "Combined" in this study means bringing two or more elements together to form a single entity

3. Results and discussion

3.1. IT

3.1.1. Distribution of Fe, Al, Si, Pb, and Cu in different particle-sized IT

The IT was classified into five size levels: +830 μm, 380–830 μm, 150–380 μm, 75–150 μm, and −75 μm. The contents of Fe, Si, Al, Pb, and Cu as shown in Fig. S1 were determined through digestion for different particle-sized IT. Fe, Al, and Si are the major constituents present in the IT. As the particle size of the IT decreased, the Fe content decreased while the Si content increased, with Al being more uniformly distributed across the different size levels of the IT, which indicates that the decreased Fe content in smaller-sized IT is mainly attributed to higher quartz content. The contents of Pb and Cu in different particle sizes of the IT are 0.13 % ~ 0.18 % and 0.15 % ~ 0.20 %, respectively. The Cu content in the + 830 μm IT was 0.15 %, while within the −830 μm range, Cu content decreased with decreasing IT particle size, a trend similar to Fe, which indicates that Cu in the IT may have certain physical or chemical associations with minerals such as limonite and hematite. The Pb content increased as the IT particle size decreased.

3.1.2. Liberations of limonite and hematite, and mineral occurrence forms of Pb and Cu

The MLA was used to determine the liberation characteristics of limonite and hematite in IT. Generally, the ore with liberation higher than 75 % has the dressing behaviour of fully liberated particle in the magnetic separation process. As depicted in Fig. 1(a), the proportions of liberation of limonite for 0–25 %, 25–50 %, 50–75 %, 75–100 %, and 100 % are 2.16 %, 3.99 %, 8.39 %, 46.17 %, and 39.29 %, respectively. The proportions of liberation of hematite for 0–25 %, 25–50 %, 50–75 %, 75–100 %, and 100 % are 6.00 %, 9.40 %, 13.9 %, 44.17 %, and 26.52 %, respectively. A comparison between the liberation proportions of the 75–100 % and 100 % reveals that the liberation of limonite exceeds that of hematite, suggesting a higher propensity for liberation of limonite within the IT (Deng et al., 2023).

The MLA was used to determine the mineral occurrence forms of Pb and Cu of IT. In Fig. 1(b), the mineral occurrence forms of Pb in IT comprise 35.55 % drugmanite, 26.55 % carminite, 13.75 % anglesite, 12.67 % limonite, 9.61 % plumbogummite, and 1.87 % stolzite. In Fig. 1 (c), the mineral occurrence forms of Cu in IT comprise 96.13 % limonite, 2.12 % chalcopyrite, and 1.75 % enargite. This indicates that Pb occurs in various mineral forms, predominantly in drugmanite and carminite. Cu is predominantly found in limonite, meaning that Cu in the IT may have certain physical or chemical associations with iron.

3.2. Enrichment of Pb Cu and Fe in MIC and NT after suspension magnetization roasting and magnetic separation

3.2.1. Suspension magnetization roasting temperature

Fig. 2 shows the MIC and NT weights and the corresponding Pb, Cu and Fe contents obtained through magnetic separation at different suspension magnetization roasting temperatures. As shown in Fig. 2(a), in the MIC, no distinct trend was observed in Pb with the increase of suspension magnetization roasting temperature. The Cu content gradually decreased from 0.31 % at 500 °C to 0.26 % at 750 °C. As shown in Fig. 2 (b), in the NT, an increasing suspension magnetization roasting temperature led to a declining trend in Cu contents. Cu decreased from 0.23 % at 500 °C to 0.12 % at 750 °C. Pb did not exhibit a noticeable change. Comparison of Fig. 2(a) and (b) shows that the Cu content in NT is lower than that in MC, indicating that Cu is more likely to exist in MIC after suspension magnetization roasting and magnetic separation. At the same time, a series of weight losses such as dehydration, dehydroxylation and clay decomposition occurred in the process of suspension magnetization roasting of IT, resulting in higher Cu and Pb content in some MIC and NT than in the IT.

As shown in Fig. 2(c), with the increase of suspension magnetization roasting temperature, the range of TFe content in MIC is 60.67–61.44 %, showing no significant trend. The TFe content in NT gradually decreases from 46.63 % at 500 °C to 22.47 % at 750 °C. As shown in Fig. 2(d), with the increase of suspension magnetization roasting temperature, the percentage of MIC obtained by magnetic separation of MP increased from 17.20 % at 500 °C to 77.40 % at 750 °C, and the percentage of NT obtained by magnetic separation of MP decreased from 82.80 % at 500 °C to 22.60 % at 750 °C. The increase in suspension magnetization roasting temperature facilitated the transformation of hematite to magnetite, resulting in an increasing proportion of Fe being separated and retained in the MIC through magnetic separation. Consequently, this led to a reduction of Fe content in the NT as the suspension magnetization roasting temperature increased.

3.2.2. Dosage of biomass pyrolysis

Fig. 3 shows the MIC and NT weights and the corresponding Pb, Cu and Fe contents obtained through magnetic separation at different dosages of biomass pyrolysis. As shown in Fig. 3(a), in the MIC, no distinct trends were observed in the proportions of Pb and Cu with

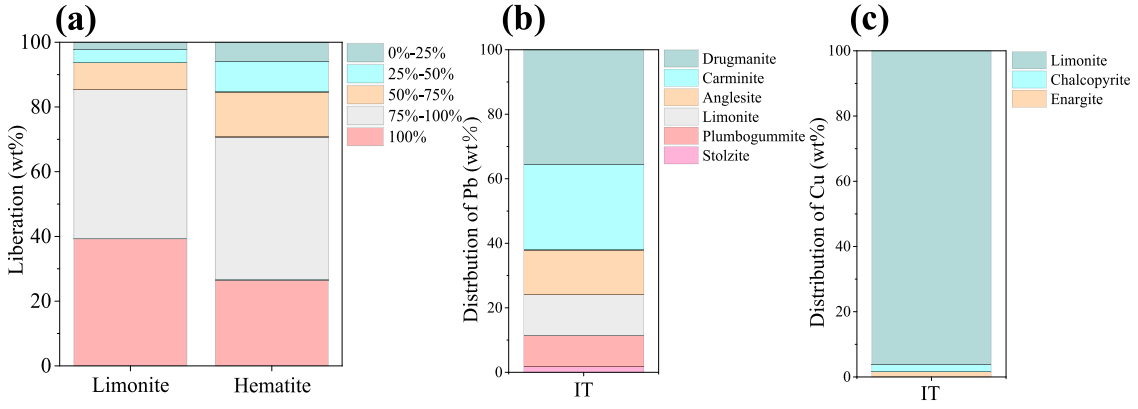

Fig. 1. (a) Liberations of limonite and hematite, and mineral occurrence forms of (b) Pb and (c) Cu.

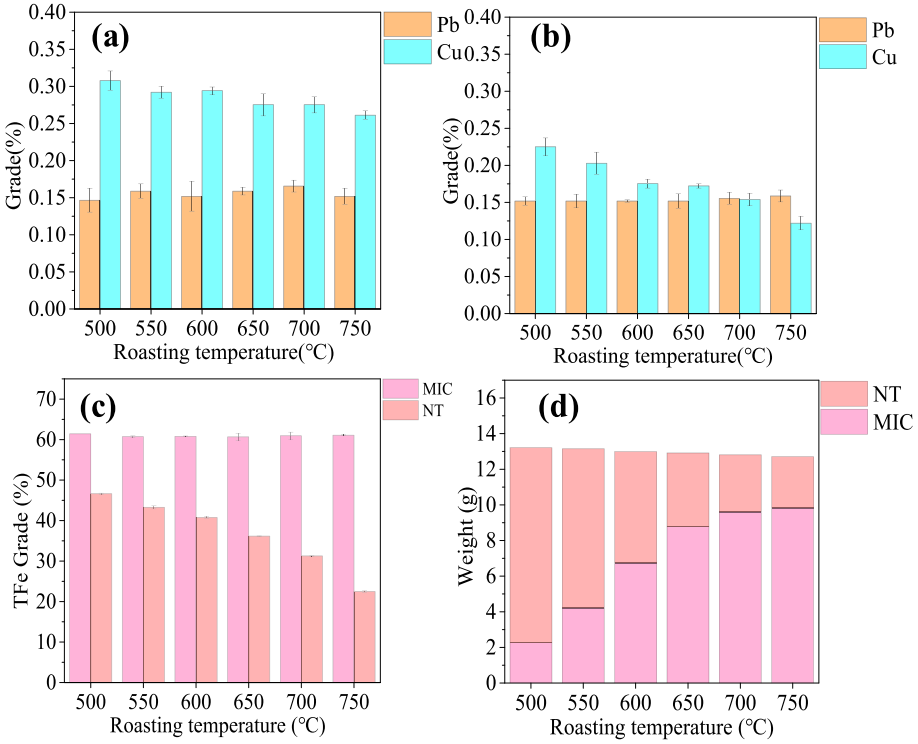

Fig. 2. Effect of suspension magnetization roasting temperature on Pb and Cu contents in (a) MIC and (b) NT; (c) effect of suspension roasting temperature on TFe content in MIC and NT; (d) effect of suspension magnetization roasting temperature on the weight of MIC and NT in the MP.

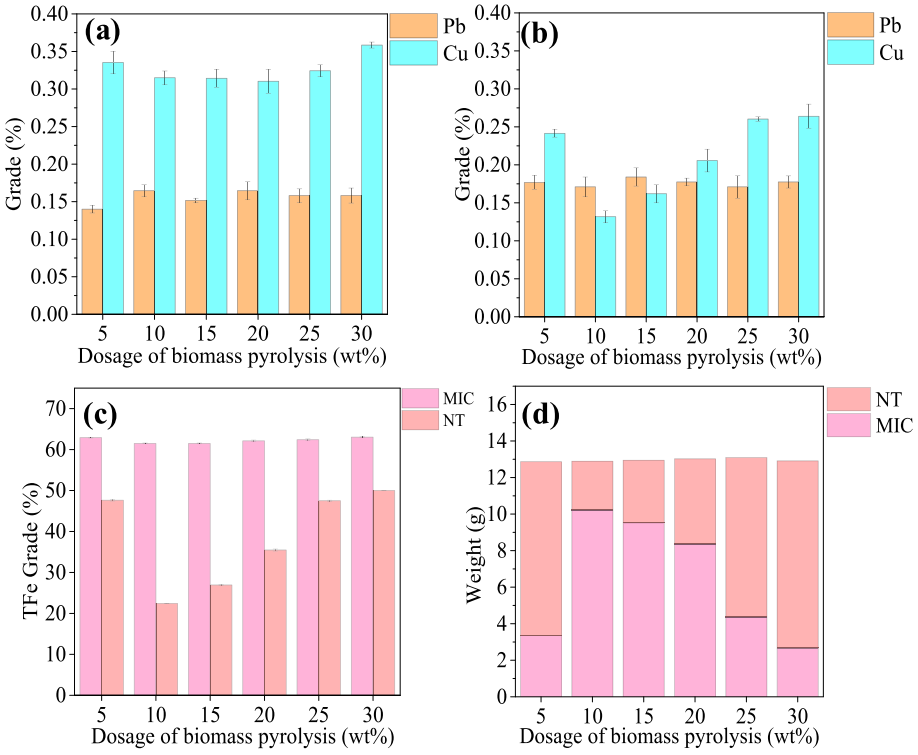

Fig. 3. Effect of dosage of biomass pyrolysis on Pb and Cu contents in (a) MIC and (b) NT; (c) effect of dosage of biomass pyrolysis on TFe content in MIC and NT; (d) effect of dosage of biomass pyrolysis on the weight of MIC and NT.

increasing dosages of biomass pyrolysis. As shown in Fig. 3(b), in the NT, with an increase in dosages of biomass pyrolysis from 5 % to 10 %, the Cu content decreased from 0.24 % to 0.13 %. Further increasing the dosage of biomass pyrolysis from 10 % to 30 %, the Cu content increased from 0.13 % to 0.26 %. The Pb content of NT exhibited no noticeable variations during the increase of dosages of biomass pyrolysis. Comparing Fig. 3(a) and (b), it can be observed that even with an increased dosage of biomass pyrolysis, the content of Cu in the MIC

remained higher than in the NT.

As shown in Fig. 3(c), as the dosage of biomass pyrolysis increased from 5 % to 10 %, the TFe content in NT decreases from 47.63 % to 22.42 %. As the dosage of biomass pyrolysis increased from 10 % to 30 %, the TFe content in NT increased from 22.42 % to 50 %. The range of TFe content in MIC is 61.50–63.04 %, showing no significant trend. As shown in Fig. 3(d), as the dosage of biomass pyrolysis increased from 5 % to 10 %, the percentage of MIC increases from 26.05 % to 79.27 %, and the percentage of NT decreases from 73.95 % to 20.73 %. As the dosage of biomass pyrolysis increased from 10 % to 30 %, the percentage of MIC decreased from 79.27 % to 20.60 %, and the percentage of NT increased from 20.73 % to 79.40 %. This indicates that when the dosage of biomass pyrolysis is less than 10 %, appropriately increasing the dosage of biomass pyrolysis can effectively promote the transformation of hematite to magnetite, and a large amount of Fe enters the MIC through magnetic separation. When the dosage of biomass pyrolysis exceeds 10 %, excessive reducing gases cause magnetite to be over reduced to non-magnetic FeO, resulting in a rapid increase in the proportion of ferrous iron in the MP. A large amount of non-magnetic FeO is lost into the NT after magnetic separation, making the Fe in the NT unable to be utilized effectively (Qiu et al., 2023). The enrichment trend of Cu in NT was consistent with that of iron, further indicating a certain correlation between Cu enrichment and iron during the suspension magnetization roasting process.

3.2.3. The enrichment ratios of Pb, Cu and Fe after suspension magnetization roasting and magnetic separation

Fig. 4 shows the enrichment ratios (E) of Pb, Cu and Fe in MIC and NT, corresponding to various suspension magnetization roasting temperatures and dosages of biomass pyrolysis. The purpose is to explore the enrichment trends of Pb, Cu and Fe after suspension magnetization roasting and magnetic separation. As shown in Fig. 4(a), the enrichment ratios of Cu and Fe at 500 °C are 1.37 and 1.32, respectively. With the increase of suspension magnetization roasting temperature, the enrichment ratios of Cu and Fe gradually increase. At 750 °C, the enrichment ratios of Cu and Fe rise to 2.14 and 3.17, respectively. This indicates that at 500 °C, Cu has already enriched in the MIC, and increasing the suspension magnetization roasting temperature can further direct it enrichment into the MIC. In Fig. 4(b), with a 5 % dosage of biomass pyrolysis, the enrichment ratios for Cu and Fe are 1.39 and 1.32. The dosage of biomass pyrolysis was increased to 10 %. This stage sees a higher conversion of hematite to magnetite without iron over-reduction. Consequently, the enrichment ratios of Cu and Fe increase to 2.39 and 3.01. This demonstrates that a controlled increase in the reduction atmosphere can specifically enhance Cu enrichment in the MIC. As the dosage of biomass pyrolysis rises to 30 %, the enrichment ratios of Cu and Fe gradually decline to 1.36 and 1.26. Beyond a 10 % dosage of biomass pyrolysis, iron over-reduction phenomena occur, which intensifies with higher dosages of biomass pyrolysis. This suggests that over-reduction of Fe inhibits Cu enrichment in the MIC, with the degree of over-reduction reaction being positively correlated with the extent of the inhibitory effect. The enrichment ratios of Cu and Fe show similar trends under different suspension magnetization roasting temperatures and dosages of biomass pyrolysis, while the enrichment ratio of Pb is close to 1, which is consistent with the results of sections 3.2.1 and 3.2.2.

3.3. Enrichment mechanism of Pb and Cu during suspension magnetization roasting and magnetic separation process

3.3.1. Enrichment mechanism of Cu

96.13 % of Cu in the IT exists in limonite, and the phase composition of this portion of Cu is unknown, so it is necessary to use chemical phase analysis to explore the phase composition of Cu. In order to explore the phase transformation of Cu during suspension magnetization roasting, a series of extractions and determinations of Cu phases was conducted on the IT. Similarly, MP, MIC and NT obtained at different suspension magnetization roasting temperatures and dosages of biomass pyrolysis were also extracted and determined. In the process of fast pyrolysis – suspension magnetization roasting, the IT is first put into the furnace body for heating operation, and then N_2 is introduced to create an inert atmosphere required for the reduction reaction. The purpose is to complete the dehydration and dehydroxylation process of IT faster, so that IT can form a porous structure and facilitate the reduction gas generated by pyrolysis to react more fully with IT. At the same time, certain oxidation conditions are created, which can reduce the S content in the IT. Therefore, the phase transition mechanism of Cu involves two environments: first oxidation and then reduction. As shown in Fig. 5(a), the proportions of free copper oxide, secondary copper sulfide, iron-manganese combined copper oxide, other combined copper oxide, and primary copper sulfide in the IT are 2.45 %, 1.70 %, 3.91 %, 0.47 %, and 91.47 %, respectively. This indicates that Cu in the IT primarily exists in the form of primary copper sulfide, with lesser proportions of copper oxide and secondary copper sulfide. At a suspension magnetization roasting temperature of 550 °C, the proportions of free copper oxide, secondary copper sulfide, iron-manganese combined copper oxide, other combined copper oxide, and primary copper sulfide in the MP are 48.06 %, 3.52 %, 9.10 %, 7.98 %, and 31.34 %, respectively. This indicates that after suspension magnetization roasting, there is a reduction in the proportion of primary copper sulfide in the MP, with a transformation towards copper oxide and secondary copper sulfide. The predominant transformation products are free copper oxide and combined copper oxide. The transformation mechanism of Cu mineral phase during suspension magnetization roasting is the oxidation of primary copper sulfide to secondary copper sulfide, the oxidation of secondary copper sulfide to free copper oxide, and the oxidation of part of free copper oxide with hematite to magnetic $CuFe_2O_4$. When N_2 does not completely occupy the furnace body, the oxygen required for the oxidation process mainly comes from air. When the furnace is filled with nitrogen, the oxygen required for the oxidation process can be obtained from hematite, which also accelerates the conversion of hematite to

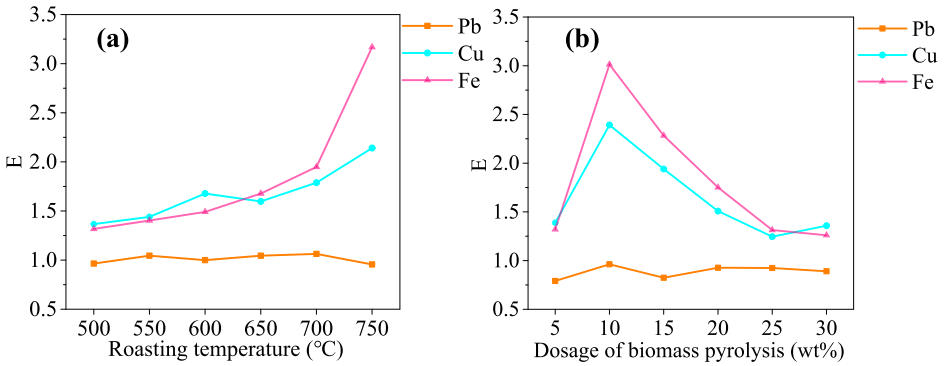

Fig. 4. Effects of (a) suspension magnetization roasting temperature and (b)dosage of biomass pyrolysis on Pb, Cu and Fe enrichment ratios (E).

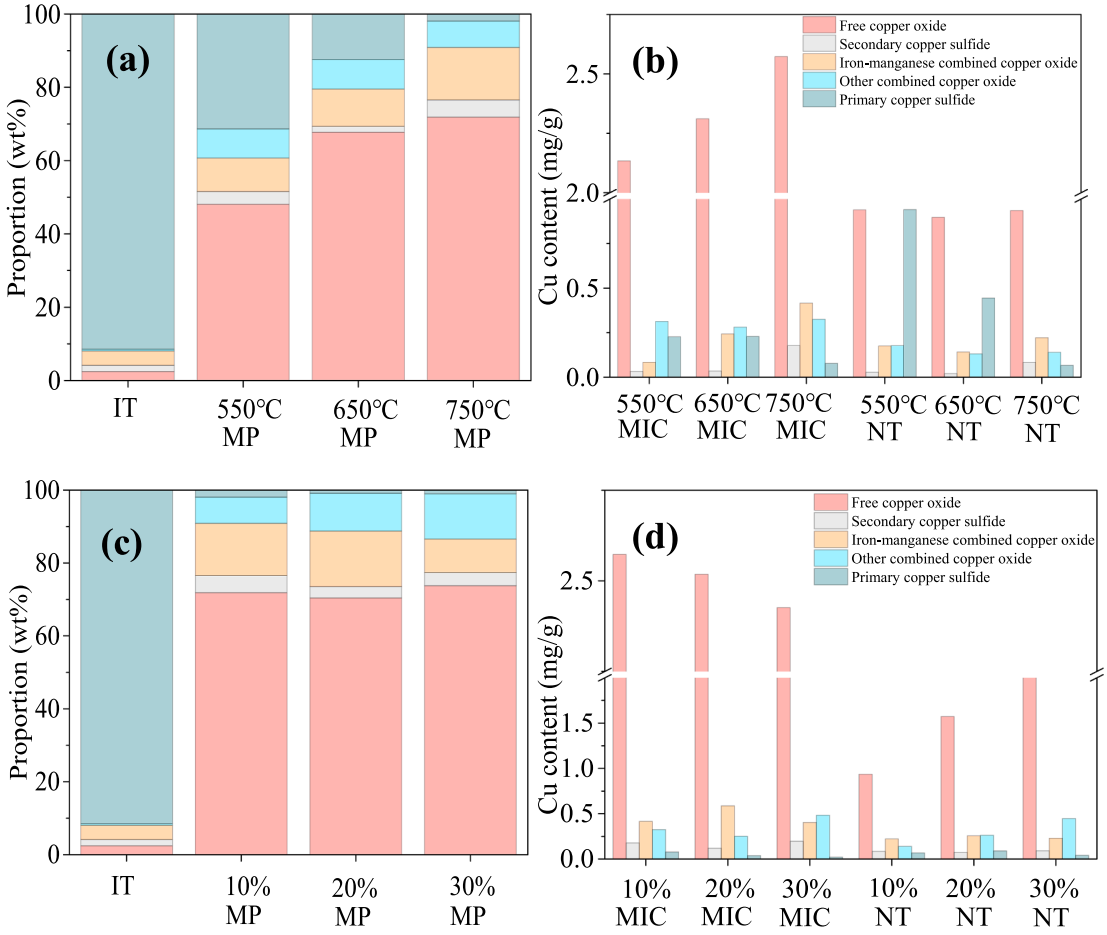

Fig. 5. (a) Cu mineral phase composition of the IT; effects of suspension magnetization roasting temperature and (c) dosage of biomass pyrolysis on the Cu mineral phase composition of the MP. (b) Effects of suspension magnetization roasting temperature and (d) dosage of biomass pyrolysis on the Cu mineral phase composition of MIC and NT.

magnetite. As the suspension magnetization roasting temperature increases from 550 °C to 750 °C, the proportions of free copper oxide and iron-manganese combined copper oxide in the MP increase from 48.06 % and 9.10 % to 71.85 % and 14.32 %, respectively, while the proportion of primary copper sulfide decreases to 5.90 %. This indicates that the increase of suspension magnetization roasting temperature effectively promotes the oxidation process of Cu, and accelerates the final transformation of primary copper sulfide into free copper oxide and iron-manganese combined copper oxide. As shown in Fig. 5(b), with the increase in suspension magnetization roasting temperature from 550 °C to 750 °C, the content of free copper oxide, secondary copper sulfide, and iron-manganese combined copper oxide in the MIC increased from 2.13, 0.03, and 0.08 mg/g to 2.57, 0.18, and 0.42 mg/g, in increasing values: free copper oxide > iron-manganese combined copper oxide > secondary copper sulfide. The increase of suspension magnetization roasting temperature effectively improves the recovery of iron and intensifies the enrichment of iron in the MIC. Since the copper sulfide in the IT is mostly associated with iron, the free copper oxide, secondary copper sulfide and iron-manganese combined copper oxide generated by the oxidation of copper sulfide are also associated with iron. Therefore, the higher the suspension magnetization roasting temperature, the higher the Cu content in the MIC. The content of primary copper sulfide in the NT decreased from 0.94 mg/g to 0.07 mg/g. The increase of suspension magnetization roasting temperature promoted the transformation of primary copper sulfide into other Cu phases, and Cu was mainly enriched in the MIC after transformation. Some fully liberated primary copper sulfide are not associated with the iron phase or gangue minerals. Thus, based on the conversion process depicted in Fig. 6, some fully liberated particles of primary copper sulfide may be converted into non-magnetic free copper oxide and retained in NT. A small amount of iron associated with primary copper sulfide was not effectively converted into magnetite and eventually enriched in the NT. With the increase in suspension magnetization roasting temperature, the TFe content decreases in the NT. Consequently, the content of primary copper sulfide in the NT is correspondingly reduced.

As shown in Fig. 5(c), with the increase in dosage of biomass pyrolysis from 10 % to 30 %, the proportion of Iron-manganese combined copper oxide in the MP decreases from 14.34 % to 9.21 %, while the proportions of free copper oxide and other combined copper oxide increase from 71.85 % and 7.18 % to 73.77 % and 12.37 %, respectively. This indicates that the higher dosage of biomass pyrolysis results in an increased presence of reducing gases, leading to the transformation of iron-manganese combined copper oxide into free copper oxide and other combined copper oxide. As shown in Fig. 5(d), in the MIC, the content of free copper oxide decreases from 2.57 to 2.42 mg/g. In the NT, the content of free copper oxide and other combined copper oxide increases from 0.94 and 0.14 mg/g to 2.00 and 0.45 mg/g, respectively. The primary copper sulfide associated with iron is transformed into free copper oxide associated with iron by suspension magnetization roasting. The increase of dosage of biomass pyrolysis increases the degree of over-reduction of iron, and a large amount of magnetite is transformed into non-magnetic FeO into NT, which is also a factor that the increase of dosage of biomass pyrolysis leads to the further enrichment of free copper oxide in the NT (Qiu et al., 2023).

The fast pyrolysis-suspension magnetization roasting system involves two reaction environments: oxidation and reduction, in which the

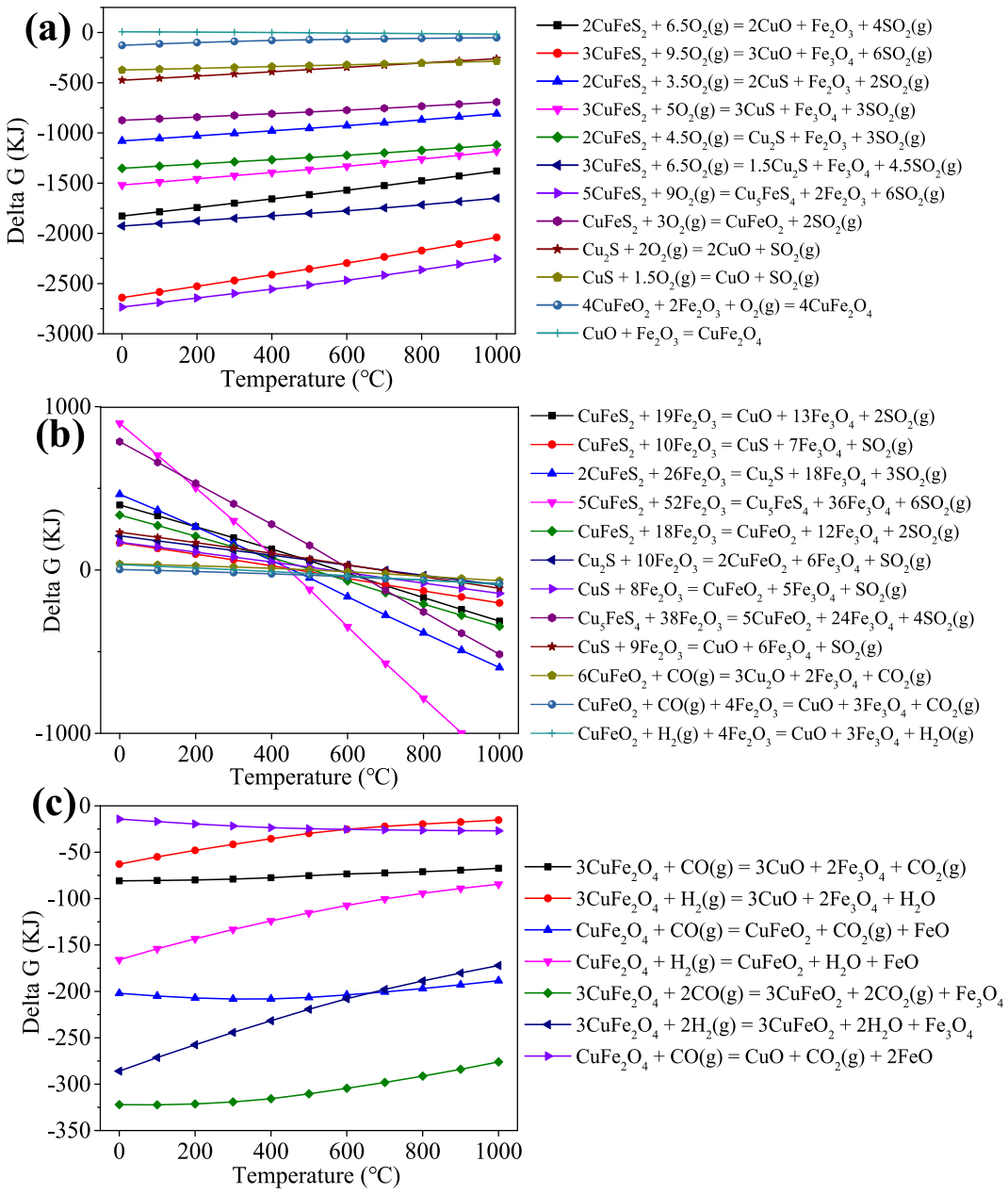

Fig. 6. Standard Gibbs free energy changes for reactions that may occur under conditions of (a) air (b) N_2 and (c) over-reduction.

oxygen in the oxidation environment comes from air, while oxygen and reducing gas in the reduction environment come from hematite and biomass pyrolysis, respectively, and all of them affect the Cu transformation in the suspension magnetization roasting process. As shown in Fig. 6, all potential chemical reactions were calculated using HSC software. As shown in Fig. 6 (a), when IT are added to a small vertical suspension furnace and air is present, oxygen participates in the reaction as the main oxide. The production of $CuFe_2O_4$ from the reaction of free copper oxide with hematite can occur at a temperature greater than 500 °C (Jiaowen et al., 2016). As shown in Fig. 6 (b), under the condition of a completely inert atmosphere and less than 10 % dosage of biomass pyrolysis, the reducing gas concentration in this stage cannot cause iron over-reduction reaction. On the one hand, hematite can be used as an oxygen carrier to provide oxygen for the conversion of primary copper sulfide to free copper oxide. On the other hand, the loss of oxygen in hematite also accelerates its own reduction reaction to achieve magnetization roasting. All reactions in this stage can occur at temperatures greater than 700 °C. As shown in Fig. 6 (c), when the dosage of biomass pyrolysis is more than 10 %, a large amount of reducing gas in this stage leads to the occurrence of iron over-reduction reaction. The decomposition reaction of $CuFe_2O_4$ with CO and H_2 produces magnetite and free copper oxide, and magnetite is further reduced to non-magnetic FeO (Liu et al., 2019). In addition, Goya et al. (1998) found that the grinding process before magnetic separation can also lead to the decomposition of copper ferrite, for example: $3CuFe_2O_4 = CuFeO_2 + Fe_3O_4 + O_2$. In summary, the conversion mechanism of copper in IT during suspension magnetization roasting is as follows: primary copper sulfide → secondary copper sulfide → free copper oxide → copper ferrite → free copper oxide.

3.3.2. *Enrichment mechanism of Pb*

MLA provides detailed mineral occurrence forms for Pb, as shown in Fig. 1(b). Chemical phase analysis focuses on identifying chemically stable or soluble forms of minerals under specific conditions, and cannot

determine detailed mineral composition information like MLA. Therefore, the enrichment trend of Pb can be explained by the mineral occurrence form of Pb in IT and the mineral association of Pb and Fe in IT. As shown in Fig. 1(b), only 12.67 % of Pb exists in the form of limonite in IT, so it is necessary to further analyse the mineral association between Pb and iron. Table. 1 shows the mineral association between Pb and iron in different forms in IT. It can be observed that the association percentages of drugmanite, carminite, anglesite, plumbogummite, stolzite with limonite and hematite are 50.98 %, 45.27 %, 7.92 %, 30.86 %, 20.91 %, respectively. Based the data in Fig. 1(b), there are 18.12 % drugmanite, 12.01 % carminite, 1.08 % anglesite, 2.96 % plumbogummite, and 0.39 % stolzite associated with iron, with an additional 12.67 % of Pb existing in the form of limonite. In total, 47.23 % of Pb is associated with iron, meaning nearly half of the Pb is associated with iron in IT, thus there is no significant relationship between the enrichment trends of Fe and Pb.

3.3.3. SEM-EDS analysis

Fig. S2 and S3 show the scanning electron microscope images and element distribution of the MIC and NT obtained under conditions of a suspension magnetization roasting temperature of 750 °C, dosage of biomass pyrolysis of 10 %, and a suspension magnetization roasting time of 10 min. Table. S3 presents the EDS analysis results for Fig. S2 and S3. The TFe grades of MIC and NT were 61.43 % and 19.28 % respectively as determined by chemical titration. The identified substances corresponding to points 1, 2, 3, 4, 5, 6, 7, 8, and 9 are Plumbogummite, magnetite, magnetite, quartz, lead-containing barium sulfate, magnetite-chlorite, iron sulfide, quartz, and white mica, respectively. The MIC contains magnetite with both Pb and Cu. There are some aluminosilicates in the MIC obtained by magnetic separation, indicating that gangue and iron are intergrown. Complete separation of gangue from iron cannot be achieved solely through magnetic separation. Meanwhile, the magnetic aggregation effect between magnetic particles may also carry some gangue into the MIC. Within the NT, there are iron minerals lost during magnetic separation, including magnetite associated with gangue and non-magnetic iron sulfide. Additionally, quartz and muscovite, along with other gangue minerals, are present in the NT. The distribution of Pb and Cu is relatively uniform in both the MIC and NT. The EDS analysis results of points 3 and 6 at MIC and NT, respectively, are Cu-bearing magnetite, which further verifies that Cu is associated with iron.

3.3.4. XRD analysis

γ-Fe_2O_3 and Fe_3O_4 have the same diffraction peaks, and the XRD analysis needs to consider the influence of γ-Fe_2O_3. γ-Fe_2O_3 will transform into stable hematite above 250 °C (Martinez et al., 1999; Wu et al., 2017). Fe_3O_4 cooled in the air below 400 °C will generate γ-Fe_2O_3 (Aliahmad and Nasiri Moghaddam, 2013; Zhang et al., 2013). Therefore, theoretically, there is no γ-Fe_2O_3 after high-temperature magnetization roasting in this study. The MP was cooled to room temperature in inert atmosphere and does not have conditions for the formation of γ-Fe_2O_3. The XRD patterns of IT, MP, MIC, and NT are shown in Fig. 7, with MP, MIC, and NT with a reaction time of 10 min. Fig. 7(a) reveals that the phase composition of IT includes Fe_2O_3, FeOOH, and SiO_2. The phases in MP obtained under the condition of 550 °C and 10 % dosage of biomass pyrolysis are Fe_2O_3, Fe_3O_4, and SiO_2, indicating that FeOOH is completely transformed into Fe_2O_3 after dehydration and dehydroxylation, but due to the low suspension magnetization roasting temperature, the transformation of Fe_2O_3 to Fe_3O_4 remains incomplete. The phases in MIC are Fe_2O_3 and Fe_3O_4, while NT consists of SiO_2, Fe_2O_3, and Fe_3O_4, indicating that magnetic separation can effectively separates gangue minerals into NT. Due to the different degrees of transformation from Fe_2O_3 to Fe_3O_4, both Fe_2O_3 and Fe_3O_4 are present in MIC and NT. Under the conditions of 750 °C and 10 % dosage of biomass pyrolysis, the phases in MP are Fe_3O_4 and SiO_2, with a notable increase in Fe_3O_4 diffraction peak intensity, indicating that under high temperature and non-overreduction conditions, all Fe_2O_3 is transformed into well-crystallized Fe_3O_4. The phases present in MIC and NT are Fe_3O_4 and SiO_2. The diffraction peak intensity of SiO_2 in NT is notably greater than that in MIC. Conversely, the diffraction peak intensity of Fe_3O_4 is lower

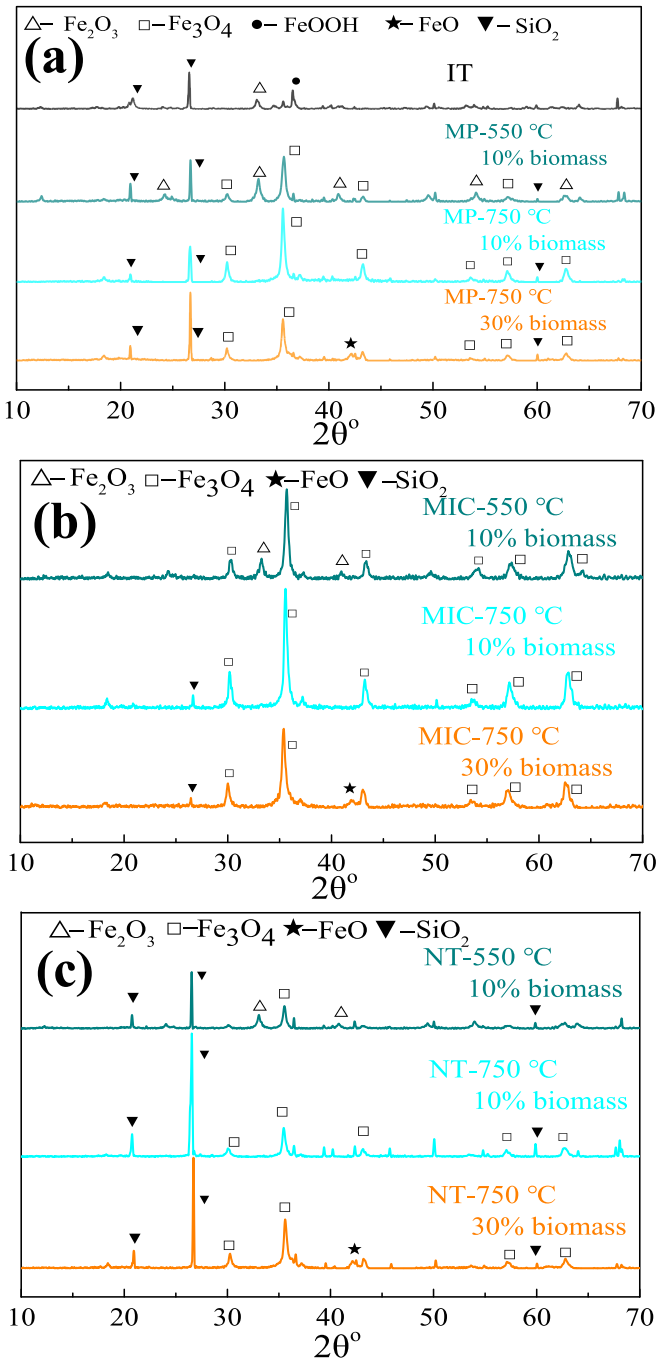

Fig. 7. XRD patterns of (a) IT and MP, (b) MIC and (c) NT.

Table 1
Mineral association of Pb and Fe in IT (wt%).

Minerals	Limonite	Hematite	Other
Drugmanite	42.68	8.30	49.02
Carminite	36.30	8.97	54.73
Anglesite	5.89	2.03	92.08
Plumbogummite	21.58	9.28	69.14
Stolzite	20.91	–	79.09

in NT compared to MIC. This suggests that the aluminosilicate in MIC cannot be completely removed by magnetic separation, and gangue and iron phases may coexist. Under the conditions of 750 °C and 30 % dosage of biomass pyrolysis, the phases in MP are Fe_3O_4, FeO, and SiO_2, with a significant decrease in the diffraction peak intensity of Fe_3O_4, indicating that under high temperature and excessive reducing gas conditions, some Fe_3O_4 is transformed into weakly magnetic FeO. The phases present in MIC and NT are Fe_3O_4, FeO and SiO_2, indicating that excessive reducing gas causes varying degrees of over-reduction of Fe_3O_4, which is also the reason for the presence of Fe_3O_4 and FeO in both MIC and NT.

3.4. Assessment of MIC quality and industrial applicability of fast pyrolysis-suspension magnetization roasting

Fe, Pb, Cu grades and Fe recovery rate of the MIC, obtained under various suspension magnetization roasting conditions in Table. S4. According to the national standard GB/T 36740–2018, the standards (mass fraction) for C60-MIC comprises 60 ≤ TFe ≤ 63 %, SiO_2 ≤ 9 %, S ≤ 0.5 %, P ≤ 0.1 %, and Al_2O_3 ≤ 2 %. If the MIC is used in blast furnace iron making, the Pb content should be less than 0.015 % according to the requirements of national standard GB 50427–2015. In this study, the contents of TFe, SiO_2, S, P, Al_2O_3, Pb, and Cu in the obtained MIC at 750 °C with a 10 % biomass pyrolysis dosage was determined as 61 %, 9.3 %, 0.27 %, 0.085 %, 4.4 %, 0.15 %, and 0.26 %, correspondingly. Therefore, Si, Al and Pb in MIC need to be further removed to meet the standards for sale and blast furnace smelting of MIC.

Magnetization roasting methods encompass shaft furnace roasting, rotary kiln roasting, fluidized bed roasting, and microwave-assisted roasting. These methods are infrequently employed in pilot-scale and industrial production due to their low product quality, high production costs, and potential for generating secondary pollution (Tang et al., 2019). Suspension (fluidized) magnetization roasting is acknowledged as the most effective and promising technology owing to its high reaction efficiency, low energy consumption, and large processing capacity (Yu et al., 2019). Continuous test results over 24 h at pilot scale to reduce siderite–hematite-mixed ore demonstrated the stability of suspension roasting. Under the conditions of a roasting temperature ranging from 525 °C to 540 °C, with CO consumption at 4.5 Nm^3/h, and N_2 consumption at 1 Nm^3/h, a TFe grade exceeding 56 %, with an average value of 57.18 %, and an iron recovery rate surpassing 91 %, with an average value of 92.22 %, were achieved (Chen et al., 2022). Furthermore, an industrial production line with an annual capacity of 1.65 million tons has been established at Jiuquan Iron and Steel Co., Ltd., China (Sun et al., 2020). Currently, suspension magnetization roasting is predominantly employed in pilot-scale or demonstration/initial commercialization of magnetization roasting, utilizing reducing gas as the reducing agent. Despite numerous experiments studying biomass as a reducing agent for magnetization roasting, its application in pilot-scale or demonstration/initial commercialization has not yet materialized (Das and Rath, 2020; Roy et al., 2020).

4. Conclusion

The enrichment of Pb, Cu, and the phase transformation mechanism of Cu in the process of suspension magnetization roasting and magnetic separation were systematically studied on the basis of fast pyrolysis-suspension magnetization roasting for iron recovery. The liberation of limonite in IT is higher than that of hematite. Pb in IT is mainly in the form of drugmanite and carminite. In IT, 96.13 % of Cu exists in limonite and is mainly in the form of primary copper sulfide. The enrichment ratios of Pb, Cu and Fe in MIC are 0.96, 2.14 and 3.17, respectively, when the suspension magnetization roasting temperature is 750 °C, the dosage of biomass pyrolysis is 10 %, and the roasting time is 10 min. 47.23 % of the Pb in IT is associated with iron, resulting in no significant enrichment trend for Pb. The increase of the suspension magnetization roasting temperature promotes the enrichment of Cu associated with iron into MIC, and the oxidation reaction of free copper oxide with Fe_2O_3 promotes the formation of magnetic copper ferrite. The increase of dosage of biomass pyrolysis is thought to lead to the over-reduction reaction of magnetite associated with Cu to form FeO, while also promoting the decomposition of magnetic copper ferrite to produce FeO and free copper oxide. The phase transformation mechanism of Cu during the suspension magnetization roasting is primary copper sulfide → secondary copper sulfide → free copper oxide → copper ferrite → free copper oxide. Cu in MIC mainly exists in two forms: copper ferrite or free copper oxide associated with magnetite. Cu in NT mainly exists in three forms: free copper oxide, fully liberated particle of primary copper sulfide or associated with FeO. This study provides theoretical guidance for the subsequent regulation and recovery of valuable metals in magnetization roasting. While magnetization roasting is relatively mature in industrial applications, the industrial application of biomass pyrolysis gasification has not yet been realized. Meanwhile, the composition of Cu phases changes after magnetization roasting, so the variation in the leaching risk of valuable metals needs to be considered in the future storage process of NT.

Funding

This study was financially supported by the Natural Science Foundation of Guangdong Province, mechanisms of deoxidation decomposition of the intergrowth minerals and silicon-aluminum activation in magnetization roasting [2024A1515010315]; the 2017 Central Special Fund for Soil, Preliminary Study on Harmless Treatment and Comprehensive Utilization of Tailings in Dabao Mountain [18HK0108].

CRediT authorship contribution statement

Guoqiang Qiu: Writing – original draft, Methodology, Investigation, Data curation. **Xunan Ning:** Writing – review & editing, Funding acquisition, Conceptualization. **Dingyuan Zhang:** Writing – review & editing, Data curation. **Jinhuan Deng:** Writing – review & editing, Data curation. **Yi Wang:** Writing – review & editing.

Declaration of competing interest

The authors declare that they have no known competing financial interests or personal relationships that could have appeared to influence the work reported in this paper.

Data availability

No data was used for the research described in the article.

Appendix A. Supplementary material

Supplementary data to this article can be found online at https://doi.org/10.1016/j.wasman.2024.05.034.

References

Aliahmad, M., Nasiri Moghaddam, N., 2013. Synthesis of maghemite (γ-Fe2O3) nanoparticles by thermal-decomposition of magnetite (Fe3O4) nanoparticles. Mater. Sci.-Poland 31 (2), 264–268. https://doi.org/10.2478/s13536-012-0100-6.

Bagatini, M.C., Kan, T., Evans, T.J., Strezov, V., 2021. Iron ore reduction by biomass volatiles. J. Sustain. Metall. 7 (1), 215–226. https://doi.org/10.1007/s40831-021-00337-3.

Beauchemin, S., Gamage McEvoy, J., Thibault, Y., MacKinnon, T., 2020. Partitioning of transition metals during magnetization of oxidized pyrrhotite tailings. Miner. Eng. 156, 106495 https://doi.org/10.1016/j.mineng.2020.106495.

Bing, L., Zhongying, Z., Biao, T., Hongbo, L., Hanchi, C., Zhen, M., 2018. Comprehensive utilization of iron tailings in China. IOP Conf. Ser.: Earth Environ. Sci. 199, 042055 https://doi.org/10.1088/1755-1315/199/4/042055.

Cao, Y., Sun, Y., Gao, P., Han, Y., Li, Y., 2021. Mechanism for suspension magnetization roasting of iron ore using straw-type biomass reductant. Int. J. Min. Sci. Technol. 31 (6), 1075–1083. https://doi.org/10.1016/j.ijmst.2021.09.008.
Cao, Z., Zhong, H., Liu, G., Zhao, S., 2009. Techniques of copper recovery from Mexican copper oxide ore. Mining Sci. Technol. (China) 19 (1), 45–48. https://doi.org/10.1016/S1674-5264(09)60009-0.
Chen, C., Han, Y., Zhang, Y., Liu, Y., Liu, Y., 2022. Efficient utilization of siderite- and hematite-mixed ore by suspension magnetization roasting: A pilot-scale study. Sustainability 14, 10353. https://doi.org/10.3390/su141610353.
Cheng, S., Han, Y., Tang, Z., Li, W., 2023. Producing magnetite concentrate from iron tailings via suspension magnetization roasting: A pilot-scale study. Sep. Sci. Technol. 58 (7), 1372–1382. https://doi.org/10.1080/01496395.2023.2189055.
Das, B., Rath, S.S., 2020. Existing and new processes for beneficiation of Indian iron ores. Trans. Indian Inst. Met. 73 (3), 505–514. https://doi.org/10.1007/s12666-020-01878-z.
Deng, J., Ning, X.A., Shen, J., Ou, W., Chen, J., Qiu, G., Wang, Y., He, Y., 2022. Biomass waste as a clean reductant for iron recovery of iron tailings by magnetization roasting. J. Environ. Manage. 317, 115435 https://doi.org/10.1016/j.jenvman.2022.115435.
Deng, J., Ning, X.-A., Qiu, G., Zhang, D., Chen, J., Li, J., Liang, Y., Wang, Y., 2023. Optimizing iron separation and recycling from iron tailings: A synergistic approach combining reduction roasting and alkaline leaching. J. Environ. Chem. Eng. 11 (3), 110266 https://doi.org/10.1016/j.jece.2023.110266.
Dengler, J.M., Hartmann, G., Jakob, H.W., Lachmann, G., 2000. Influence of tramp elements in the steel on the castability and deformation behaviour of beam blanks.
EPA, U., 1996. Method 3052: Microwave Assisted and Digestion of Siliceous and Organically Based Matrices. Washington, DC, USA.
Goya, G.F., Rechenberg, H.R., Jiang, J.Z., 1998. Structural and magnetic properties of ball milled copper ferrite. J. Appl. Phys. 84 (2), 1101–1108. https://doi.org/10.1063/1.368109.
Hong, J.H., Lee, S.H., Kim, J.G., Yoon, J.B., 2012. Corrosion behaviour of copper containing low alloy steels in sulphuric acid. Corros. Sci. 54, 174–182. https://doi.org/10.1016/j.corsci.2011.09.012.
Jiao, K.X., Zhang, J.L., Liu, Z.J., Chen, C.L., Liu, F., 2016. Circulation and accumulation of harmful elements in blast furnace and their impact on the fuel consumption. Ironmak. Steelmak. 44 (5), 344–350. https://doi.org/10.1080/03019233.2016.1210913.
Jiaowen, S., Kim, D.W., Kim, S.B., Jo, Y.M., 2016. CO_2 decomposition using metal ferrites prepared by co-precipitation method. Korean J. Chem. Eng. 33 (11), 3162–3168. https://doi.org/10.1007/s11814-016-0192-5.
Li, W.S., Lei, G.Y., Xu, Y., Huang, Q.F., 2018. The properties and formation mechanisms of eco-friendly brick building materials fabricated from low-silicon iron ore tailings. J. Clean Prod. 204, 685–692. https://doi.org/10.1016/j.jclepro.2018.08.309.
Li, N., Lo, S., Hu, C., Hsieh, C., Chen, C., 2011. Stabilization and phase transformation of $CuFe_2O_4$ sintered from simulated copper-laden sludge. J. Hazard. Mater. 190 (1), 597–603. https://doi.org/10.1016/j.jhazmat.2011.03.089.
Li, C., Sun, H., Bai, J., Li, L., 2010. Innovative methodology for comprehensive utilization of iron ore tailings: part 1. The recovery of iron from iron ore tailings using magnetic separation after magnetizing roasting. J. Hazard. Mater. 174 (1–3), 71–77. https://doi.org/10.1016/j.jhazmat.2009.09.018.
Liu, F., Liu, J., Yang, Y., Wang, Z., Zheng, C., 2019. Reaction mechanism of spinel $CuFe_2O_4$ with CO during chemical-looping combustion: An experimental and theoretical study. Proc. Combust. Inst. 37 (4), 4399–4408. https://doi.org/10.1016/j.proci.2018.06.222.
Liu, P., Yuan, S., Sun, Y., Han, Y., Gao, P., Li, Y., 2022. An efficient and green method to separate iron and manganese from ferromanganese ore by suspension magnetization roasting and magnetic separation. Powder Technol. 402 https://doi.org/10.1016/j.powtec.2022.117359.
Lyu, Z., Chai, J., Xu, Z., Qin, Y., Cao, J., 2019. A comprehensive review on reasons for tailings dam failures based on case history. Adv. Civ. Eng. 2019, 1–18. https://doi.org/10.1155/2019/4159306.
Martinez, N., Williams, A.J., Seyyed Ebrahimi, S.A., Harris, I.R., 1999. A study of the evolution of the constituent phases and magnetic properties of hydrogen-treated Sr-hexaferrite during calcination. J. Mater. Sci. 34 (10), 2401–2406. https://doi.org/10.1023/A:1004506514713.
Mustafa, S., Liqun, L., Christophe, N.J., Bo-tao, Z., Chen-xi, W., Yanming, L., Yang, L., Ting, J., Kabashi, M., 2023. Novelty on deep reduction roasting through removal of lead and zinc impurities from iron ore afore ironmaking. Powder Technol. 428, 118857 https://doi.org/10.1016/j.powtec.2023.118857.
Nunna, V., Hapugoda, S., Eswarappa, S.G., Raparla, S.K., Pownceby, M.I., Sparrow, G.J., 2020. Evaluation of dry processing technologies for treating low grade lateritic iron ore fines. Miner. Process. Extr. Metall. Rev. 43, 283–299. https://doi.org/10.1080/08827508.2020.1837127.
Nwachukwu, C.M., Wang, C., Wetterlund, E., 2021. Exploring the role of forest biomass in abating fossil CO_2 emissions in the iron and steel industry – The case of Sweden. Appl. Energy 288, 116558. https://doi.org/10.1016/j.apenergy.2021.116558.
Qiu, G., Ning, X., Shen, J., Wang, Y., Zhang, D., Deng, J., 2023. Recovery of iron from iron tailings by suspension magnetization roasting with biomass-derived pyrolytic gas. Waste Manag. 156, 255–263. https://doi.org/10.1016/j.wasman.2022.11.034.
Roy, S.K., Nayak, D., Rath, S.S., 2020. A review on the enrichment of iron values of low-grade Iron ore resources using reduction roasting-magnetic separation. Powder Technol. 367, 796–808. https://doi.org/10.1016/j.powtec.2020.04.047.
Sun, Y., Zhu, X., Han, Y., Li, Y., 2019. Green magnetization roasting technology for refractory iron ore using siderite as a reductant. J. Clean Prod. 206, 40–50. https://doi.org/10.1016/j.jclepro.2018.09.113.
Sun, Y., Zhu, X., Han, Y., Li, Y., Gao, P., 2020. Iron recovery from refractory limonite ore using suspension magnetization roasting: A pilot-scale study. J. Clean Prod. 261, 121221 https://doi.org/10.1016/j.jclepro.2020.121221.
Tang, Z.D., Gao, P., Han, Y.X., Guo, W., 2019. Fluidized bed roasting technology in iron ores dressing in China: A review on equipment development and application prospect. J. Min. Metall. Sect. B. 55 (3), 295–303. https://doi.org/10.2298/jmmb190520051t.
Trinkel, V., Aschenbrenner, P., Thaler, C., Rechberger, H., Mallow, O., Fellner, J., 2017. Distribution of Zn, Pb, K, and Cl in blast furnace lining. Steel Res. Int. 88 (1), 1600153. https://doi.org/10.1002/srin.201600153.
USGS, 2023. Iron ore, Mineral Commodity Summaries U.S. Geological Survey, pp. 98–99.
Vasile, A., Miläşan, A.R., Andrei, A.E., Turcu, R.N., Drăgoescu, M.F., Axinte, S., Mihaly, M., 2021. An integrated value chain to iron-containing mine tailings capitalization by a combined process of magnetic separation, microwave digestion and microemulsion – assisted extraction. Process Saf. Environ. Prot. 154, 118–130. https://doi.org/10.1016/j.psep.2021.08.012.
Wang, G., Liu, Y., Tong, L., Jin, Z., Chen, G., Yang, H., 2019. Effect of temperature on leaching behavior of copper minerals with different occurrence states in complex copper oxide ores. Trans. Nonferrous Met. Soc. Chin. 29 (10), 2192–2201. https://doi.org/10.1016/S1003-6326(19)65125-3.
Wu, F., Cao, Z., Wang, S., Zhong, H., 2017. Phase transformation of iron in limonite ore by microwave roasting with addition of alkali lignin and its effects on magnetic separation. J. Alloy. Compd. 722, 651–661. https://doi.org/10.1016/j.jallcom.2017.06.142.
Wu, F., Cao, Z., Wang, S., Zhong, H., 2018. Novel and green metallurgical technique of comprehensive utilization of refractory limonite ores. J. Clean Prod. 171, 831–843. https://doi.org/10.1016/j.jclepro.2017.09.198.
Xiao-Feng, J., Fei, T., Qing-Hua, L., Center, T.J.Y.G., 2016. The auomic absorption spectrography of Cu testing in phase analysis of Cu ore. Yunnan Geol. 35 (4), 514–516.
Yu, J., Han, Y., Li, Y., Gao, P., 2019. Recent advances in magnetization roasting of refractory iron ores: A technological review in the past decade. Miner. Process. Extr. Metall. Rev. 41 (5), 349–359. https://doi.org/10.1080/08827508.2019.1634565.
Yuan, S., Zhou, W., Han, Y., Li, Y., 2020. Individual enrichment of manganese and iron from complex refractory ferromanganese ore by suspension magnetization roasting and magnetic separation. Powder Technol. 373, 689–701. https://doi.org/10.1016/j.powtec.2020.07.005.
Yuan, S., Wang, R., Zhang, Q., Li, Y., Gao, P., 2022. Extraction and phase transformation of iron in fine-grained complex hematite ore by suspension magnetizing roasting and magnetic separation. Korean J. Chem. Eng. 39 (7), 1891–1901. https://doi.org/10.1007/s11814-022-1116-1.
Zhang, H., Chen, G., Cai, X., Fu, J., Liu, M., Zhang, P., Yu, H., 2021. The leaching behavior of copper and iron recovery from reduction roasting pyrite cinder. J. Hazard. Mater. 420, 126561 https://doi.org/10.1016/j.jhazmat.2021.126561.
Zhang, X., Niu, Y., Meng, X., Li, Y., Zhao, J., 2013. Structural evolution and characteristics of the phase transformations between α-Fe_2O_3, Fe_3O_4 and γ-Fe_2O_3 nanoparticles under reducing and oxidizing atmospheres. CrstEngComm 15 (40), 8166–8172. https://doi.org/10.1039/C3CE41269E.
Zhang, Q., Sun, Y., Han, Y., Li, Y., 2020. Pyrolysis behavior of a green and clean reductant for suspension magnetization roasting. J. Clean Prod. 268, 122173 https://doi.org/10.1016/j.jclepro.2020.122173.
Zhang, Q., Sun, Y., Wang, S., Han, Y., Li, W., Li, Y., 2022. Whether magnetization roasting requires complete phase reconstruction of iron minerals: A study of phase transition and microstructure evolution. Powder Technol. 411 https://doi.org/10.1016/j.powtec.2022.117934.
Zhang, N., Tang, B., Liu, X., 2021. Cementitious activity of iron ore tailing and its utilization in cementitious materials, bricks and concrete. Constr. Build. Mater. 288, 123022 https://doi.org/10.1016/j.conbuildmat.2021.123022.
Zhao, Q., Wei, J., 2020. Zero-waste recycling method for textile dyeing sludge by magnetizing roasting–magnetic separation process and ceramic filter preparation. Chem. Pap. 74 (12), 4389–4399. https://doi.org/10.1007/s11696-020-01249-4.
Zhu, X., Han, Y., Sun, Y., Li, Y., Wang, H., 2020. Siderite as a novel reductant for clean utilization of refractory iron ore. J. Clean Prod. 245, 118704 https://doi.org/10.1016/j.jclepro.2019.118704.